# Calcium Currents in the A7r5 Smooth Muscle–derived Cell Line

## Calcium-dependent and Voltage-dependent Inactivation

BARTOLO GIANNATTASIO, STEPHEN W. JONES, and ANTONIO SCARPA

From the Department of Physiology and Biophysics, Case Western Reserve University, Cleveland, Ohio 44106

ABSTRACT    Inactivation of a dihydropyridine-sensitive calcium current was studied in a cell line (A7r5) derived from smooth muscle of the rat thoracic aorta. Inactivation is faster with extracellular $Ca^{2+}$ than with $Ba^{2+}$. In $Ba^{2+}$, inactivation increases monotonically with depolarization. In $Ca^{2+}$, inactivation is related to the amount of inward current, so that little inactivation is seen in $Ca^{2+}$ for brief depolarizations approaching the reversal potential. Longer depolarizations in $Ca^{2+}$ reveal two components of inactivation, the slower component behaving like that observed in $Ba^{2+}$. Furthermore, lowering extracellular $Ca^{2+}$ slows inactivation. These results are consistent with the coexistence of two inactivation processes, a slow voltage-dependent inactivation, and a more rapid current-dependent inactivation which is observable only with $Ca^{2+}$. $Ca^{2+}$-dependent inactivation is decreased but not eliminated when intracellular $Ca^{2+}$ is buffered by 10 mM BAPTA, suggesting that $Ca^{2+}$ acts at a site on or near the channel. We also studied recovery from inactivation after either a short pulse (able to produce significant inactivation only in $Ca^{2+}$) or a long pulse (giving similar inactivation with either cation). Surprisingly, recovery from $Ca^{2+}$-dependent inactivation was voltage dependent. This suggests that the pathways for recovery from inactivation are similar regardless of how inactivation is generated. We propose a model where $Ca^{2+}$- and voltage-dependent inactivation occur independently.

## INTRODUCTION

Two primary mechanisms of inactivation have been described for calcium channels: voltage-dependent and $Ca^{2+}$-dependent inactivation (Eckert and Chad, 1984; Carbone and Swandulla, 1989). $Ca^{2+}$-dependent inactivation is greatly decreased when $Ca^{2+}$ is replaced by $Ba^{2+}$, and can often be prevented by buffering intracellular $Ca^{2+}$. Usually, $Ca^{2+}$-dependent inactivation is maximal near the voltage that generates peak

inward current and inactivation decreases at more positive potentials, but this is neither necessary (Gutnick et al., 1989) nor sufficient (Jones and Marks, 1989) to demonstrate $Ca^{2+}$ dependence. Voltage- and $Ca^{2+}$-dependent inactivation mechanisms coexist in many cell types (Brown et al., 1981; Kass and Sanguinetti, 1984; Lee et al., 1985; Satin and Cook, 1989), including smooth muscle (Jmari et al., 1986; Ganitkevich et al., 1987).

Entry of $Ca^{2+}$ through dihydropyridine-sensitive calcium channels is critical for arterial smooth muscle tone (Nelson et al., 1990). Inactivation of calcium channels could play an important role in regulation of channel availability, but there is little information on the kinetics and mechanisms of calcium channel inactivation in such cells.

We demonstrate in A7r5 cells that two separable mechanisms of inactivation coexist, one dependent on membrane potential and the other on $Ca^{2+}$ entry. $Ca^{2+}$ appears to act locally to inactivate the channel through which it enters (Mazzanti and DeFelice, 1990; Yue et al., 1990), not diffusely by increasing cytosolic $Ca^{2+}$ (Gutnick et al., 1989). We propose a model for calcium current inactivation that explains the major features of our results.

Preliminary reports of some of these results have appeared in abstract form (Giannattasio et al., 1989, 1990).

## METHODS

### Voltage Clamp

A7r5 cells (Kimes and Brandt, 1976) were cultured as described (Marks et al., 1990). Currents were recorded in the whole-cell configuration using an Axopatch 1B (Axon Instruments, Inc., Foster City, CA) or List EPC 7 (List Medical, Darmstadt/Eberstadt, Germany) amplifier. We used electrodes with series resistances of 2–5 M$\Omega$, as estimated from cancellation of the capacity transient. Series resistance errors should therefore have been <5 mV for the <1-nA currents studied here. Spherical cells with smooth surfaces, no evident membrane folding, and few visible surface attachments, were selected to reduce space clamp errors. Despite these precautions, some cells showed signs of slow voltage clamp, including large residual capacity transients after optimal compensation. Other cells appeared to be excellently clamped, with rapid ($\tau < 1$ ms) tail currents (Obejero-Paz et al., 1990). In cells studied here, the currents induced by depolarizing steps were well controlled, with graded activation and no "notches."

pClamp software (version 5; Axon Instruments, Inc.) was used with IBM AT-compatible microcomputers to both generate voltage commands and acquire data. Records were generally analog filtered at 5 kHz (depending on the sampling rate) and then digitally filtered during the analysis at 1 kHz. Analysis was also done with pClamp (Clampan and Clampfit programs). Leak subtraction was done either by adding the inverted and scaled currents generated by ¼ amplitude hyperpolarizing pulses, or by using values from linear regression of currents generated by hyperpolarizing pulses. Further analysis was done with Lotus 1-2-3 and figures were prepared with Micrografx Draw Plus.

### Solutions and Materials

The standard extracellular solution contained (in mM): 112.5 NaCl, 5 KCl, 1.2 MgCl$_2$, 10 CaCl$_2$ or BaCl$_2$, 2.5 NaHEPES, and 10 glucose, adjusted to pH 7.4 with NaOH. When necessary, NaCl was osmotically substituted for CaCl$_2$ or BaCl$_2$. The standard intracellular solution contained (in

mM): 120 CsCl, 4 MgCl$_2$, 5 TrisATP, 1 CsEGTA, and 2.5 CsHEPES, adjusted to pH 7.2 with CsOH. Where noted, CsEGTA was varied from 0 to 10 mM, or substituted with 1–10 mM CsBAPTA, with changes in CsCl to maintain osmolarity. The extracellular solution was changed using a gravity flow system controlled remotely by solenoid valves.

EGTA (ethyleneglycol-bis-[*b*-aminoethyl ether] *N,N,N',N'*-tetraacetic acid), HEPES (*N*-(2-hydroxyethyl)piperazine-*N'*-[2-ethanesulfonic acid]), and ATP (Na or Tris salt) were purchased from Sigma Chemical Co. (St. Louis, MO). BAPTA (1,2-bis[2-aminophenoxy]ethane-*N,N,N',N'*-tetraacetic acid) was from Sigma Chemical Co. (free acid) or Molecular Probes, Inc. (Eugene, OR) (cesium salt). Other chemicals were reagent grade.

### Isolation and Stability of Calcium Current

The predominant voltage-dependent current in A7r5 cells is a dihydropyridine-sensitive (L-type) calcium current (Marks et al., 1990). With intracellular CsCl, we did not observe any time-dependent outward current, even for >300-ms steps to strongly depolarized voltages (+40 to +70 mV). Replacement of internal and/or external monovalent cations with *N*-methyl D-glucamine did not modify the current profile. In some cells a transient (T) current was present, but it was absent or <10% of the total current in the cells reported here. The normal holding potential (−60 mV) was changed to −40 or −50 mV (as noted) when T current had been observed recently.

The amplitude of current, and the extent of rundown with time, varied widely among cells. Many cells were rejected due to small (<50 pA) initial currents. But in many cases, with internal MgATP and EGTA, calcium currents could be recorded for >1 h. Rundown appeared to be faster without EGTA or BAPTA, and with long and frequent depolarizing pulses.

### Computer Modeling

The AXOVACS programs (Axon Instruments, Inc.) were modified to simulate calcium currents. Other programs were written in QuickBASIC (Microsoft, Redmond, WA) to calculate properties of the models, using in part the analytic solution to the general three-state cyclic model (Gutnick et al., 1989).

RESULTS

### Inactivation

Inactivation is faster in Ca$^{2+}$ than in Ba$^{2+}$ (Figs. 1 and 2). Inactivation can be observed either as the time-dependent decrease of inward current during a maintained depolarization, or as a decrease of the peak current generated by a second test pulse in a double pulse experiment (Eckert and Tillotson, 1981). A 60-ms prepulse generates ~50% inactivation in Ca$^{2+}$ but only ~10% in Ba$^{2+}$ (Fig. 1). Maximal inactivation in Ca$^{2+}$ is observed with prepulses giving maximal inward current, with less inactivation at more positive voltages. Therefore, except where noted, inactivation was measured at the voltage producing peak inward current (usually +20 mV in 10 mM Ca$^{2+}$, and +10 mV in 1 mM Ca$^{2+}$ or 10 mM Ba$^{2+}$).

Longer prepulses (330 ms) in Ba$^{2+}$ produced 32 ± 4% inactivation (mean ± SEM, $n = 14$) (Fig. 2). The range was 22–50%, except for one cell that showed no inactivation (see McCarthy and Cohen, 1989). In Ba$^{2+}$, inactivation increases almost monotonically with voltage. The same pulse length with Ca$^{2+}$ produces maximal inactivation for prepulses giving maximal inward current, but a considerable amount
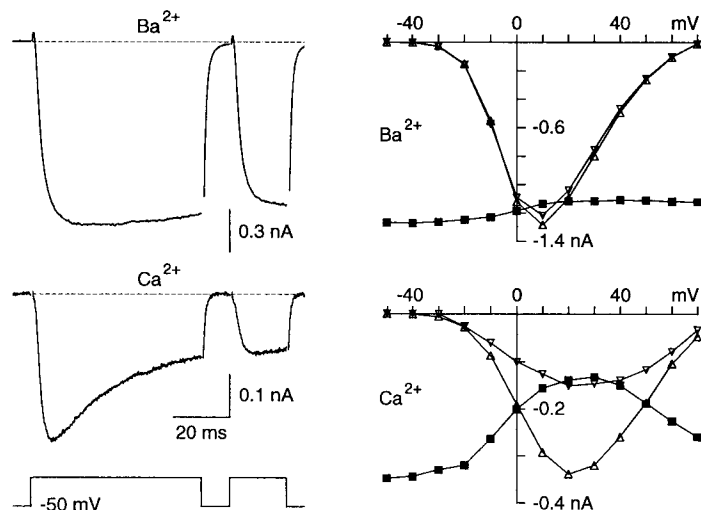
FIGURE 1.    Inactivation of calcium current generated by short depolarizations in A7r5 cells. 60-ms depolarizing prepulses of variable amplitude were given to induce inactivation, followed by a second constant pulse to the voltage giving maximal inward current ($+10$ mV in 10 mM $Ba^{2+}$ and $+20$ mV in 10 mM $Ca^{2+}$) to assay inactivation. At the left, leak-subtracted currents are shown (filtered at 5 kHz) for the records where the prepulse and postpulse voltages were equal. Current–voltage relations are shown at the right. Currents were measured at the peak current during the prepulse ($\triangle$), at the end of the prepulse ($\triangledown$), and at peak current during the test pulse ($\blacksquare$). The current–voltage curves shown are averages of two protocols, with prepulse voltages given in ascending and descending order, to compensate for rundown. Rundown, measured as the decrease in peak current between the two runs, was $<3\%$.
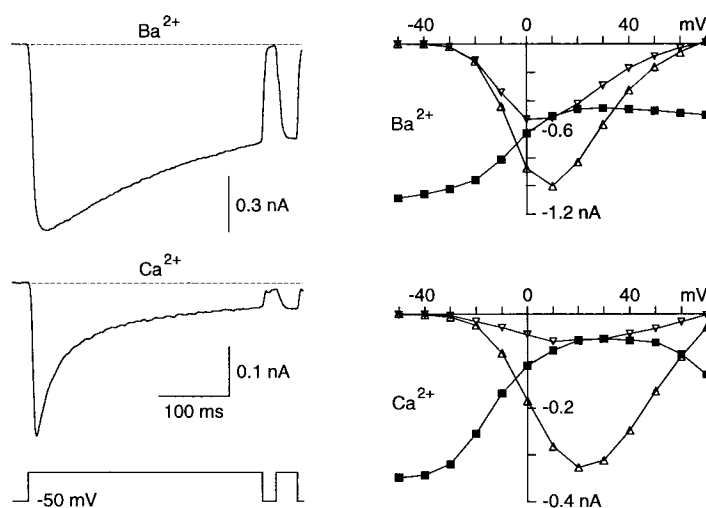


FIGURE 2.    Inactivation of calcium current generated by longer depolarizations. Protocols as in Fig. 1, except that prepulses lasted 330 ms, and records were filtered at 100 Hz. The data for Figs. 1 and 2 were recorded from the same cell, $\sim 50$ min ($Ba^{2+}$) and $\sim 80$ min ($Ca^{2+}$) after the start of whole-cell dialysis. Rundown was 11% in $Ca^{2+}$ and 35% in $Ba^{2+}$.

of inactivation also occurs at more depolarized voltages. Inactivation was considerably slower in $Ba^{2+}$ than in $Ca^{2+}$ in nine of nine cells tested under both conditions.

The relation of current to inactivation is examined more directly, using normalized values, in Fig. 3. Inactivation closely parallels the current for short prepulses in $Ca^{2+}$ (Fig. 3 A). In $Ba^{2+}$, inactivation parallels the increase in current at negative voltages, but strong depolarizations that do not generate large currents also reduce the postpulse (Fig. 3 C). For long prepulses in $Ca^{2+}$, the inactivation curve is broadened, with considerable inactivation at voltages producing little inward current (Fig. 3 B).
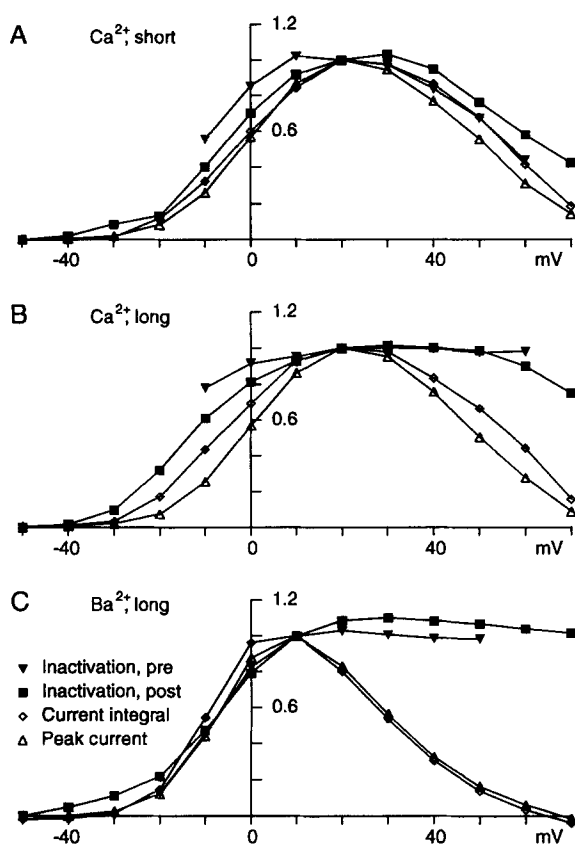


FIGURE 3. Normalized currents and inactivation, from the data of Figs. 1 and 2. Currents (△) and current integrals (◇) were normalized to values at peak inward current. Inactivation was measured in two ways, from the decline in current during the prepulse (▼; current at the end of the pulse divided by the peak current at that voltage), and from the postpulse amplitude (■; divided by the postpulse amplitude when no prepulse was given). The fractional inactivation measured in either way was then normalized to the fractional inactivation measured at the voltage generating maximal inward current. Inactivation during the prepulse was calculated only for voltages where the current was at least 20% of the maximum. The analysis for $Ba^{2+}$ after 60-ms prepulses is not shown since the amount of inactivation generated during that protocol was very small.

The broadening is especially clear at more depolarized voltages, whether inactivation is compared with peak current or with the integral of $Ca^{2+}$ entry during the entire prepulse.

Inactivation measured by the postpulse agrees well with inactivation during the prepulse for voltages where the prepulse current is large enough for its inactivation to be accurately measured (Fig. 3). This is additional evidence that the calcium current is well isolated, and that we are measuring inactivation rather than unrelated phenomena such as activation of an outward current. Thus, the time course of

inactivation can be measured directly from the amplitude of the current during the prepulse (Fig. 4).

### Inactivation Kinetics

The time course of inactivation during a 60-ms pulse in $Ca^{2+}$ could be well fitted by a single exponential (Fig. 4 A). Similar rapid inactivation ($\tau$ = 15–45 ms) was observed in 20 of 26 cells tested in $Ca^{2+}$. In contrast, a good fit to the time course of inactivation during a 330-ms pulse in $Ca^{2+}$ required the sum of two exponentials of similar amplitude (Fig. 4, C and D). In $Ba^{2+}$ one exponential fit the time course of inactivation (Fig. 4 B), with time constant 210 ± 13 ms ($n$ = 20, range 120–343 ms).
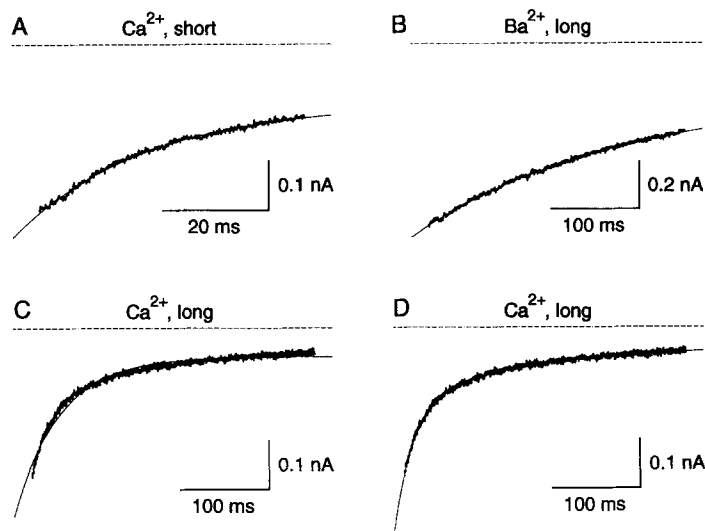


FIGURE 4. The time course of inactivation. Currents (thick traces) were fitted to single exponentials (thin traces) during (A) a 60-ms depolarization to +20 mV in $Ca^{2+}$ ($\tau$ = 24.5 ms), (B) a 330-ms depolarization to +10 mV in $Ba^{2+}$ ($\tau$ = 232 ms), and (C) a 330-ms depolarization to +20 mV in $Ca^{2+}$ ($\tau$ = 50.2 ms) from the same cell as Figs. 1–3. (D) A fit of the sum of two exponentials ($\tau$ = 21.5 ms, amplitude 0.15 nA; $\tau$ = 139 ms, amplitude 0.11 nA) to the data of C. Dashed lines indicate zero current.

The difference in inactivation rates allows selective generation of $Ca^{2+}$- and voltage-dependent inactivation: 60-ms pulses in $Ca^{2+}$ generate predominantly $Ca^{2+}$-mediated inactivation, whereas 330-ms pulses in $Ba^{2+}$ generate inactivation that appears to depend solely on voltage (Figs. 1–3). Fig. 5 plots time constants measured for each condition at different voltages. The fast component in $Ca^{2+}$ is fastest at or near the voltage producing peak current, suggesting current dependence. In $Ba^{2+}$, a slight increase in inactivation rate occurs at more depolarized voltages. The faster time constant measured from 330-ms pulses in $Ca^{2+}$ is also dependent on current and is slightly faster (5–10 ms) than the single time constant fit to short pulses. The slower time constant in $Ca^{2+}$ is more variable, and two time constants are not always well resolved at more depolarized voltages.
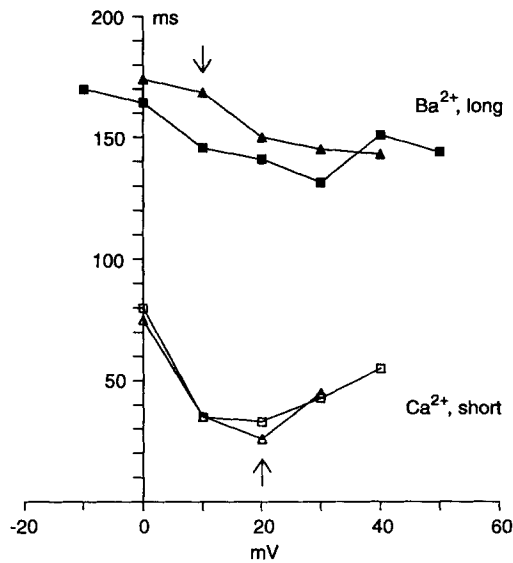
FIGURE 5. Inactivation time constants. Each symbol is a different cell. Values are from single exponential fits to currents during 330-ms steps (*solid symbols*, $Ba^{2+}$) or 60-ms steps (*open symbols*, $Ca^{2+}$). The arrows mark the voltage inducing peak inward current under each condition. Only a narrow voltage range could be examined, where the current was large enough and sufficient inactivation occurred. We found a ~10-mV variation in the position of peak current for different cells in the same conditions, but generally the fast time constant in $Ca^{2+}$ was the fastest at or slightly hyperpolarized to peak current, with slower values on both sides.

## Dependence on Intracellular Calcium

The preceding results suggest the coexistence of two inactivation processes, one fast (~20 ms) and dependent on $Ca^{2+}$ entry, one slower (~200 ms) and voltage dependent. We tested this hypothesis with procedures designed to modulate the $Ca^{2+}$-dependent component: changing the level of intracellular $Ca^{2+}$ buffer, and decreasing the current with low $[Ca^{2+}]_o$.

Inactivation was similar with 1 or 10 mM EGTA, or with no added calcium buffer. Inactivation rates in $Ca^{2+}$ with 10 mM BAPTA were generally slower than with 1 mM EGTA, but clearly faster than with $Ba^{2+}$ (Fig. 6). From fits with two exponentials, the faster time constant for inactivation was 21 ± 2 ms ($n$ = 3) with 1 mM EGTA, and
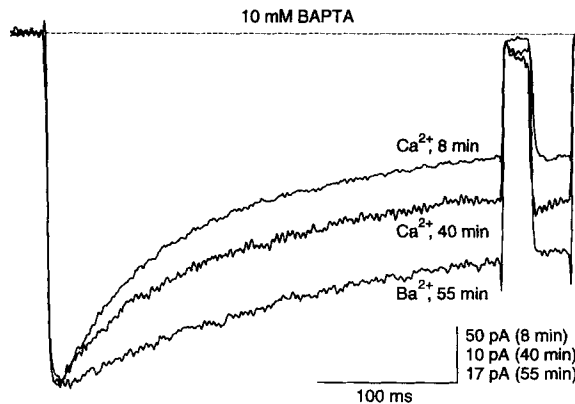


FIGURE 6. Effect of 10 mM intracellular BAPTA on calcium current inactivation. Currents (filtered at 200 Hz) were from voltage steps to the point of peak inward current (+20 mV in $Ca^{2+}$, +10 mV in $Ba^{2+}$) from the holding potential of −50 mV, recorded at the times indicated. Currents were scaled to the peak current for each record.

$40 \pm 3$ ms ($n = 3$) with 10 mM BAPTA, in one batch of cells. Single exponential fits to inactivation during 60-ms pulses gave time constants of $41 \pm 3$ ms ($n = 8$) with BAPTA. $Ca^{2+}$-dependent inactivation could still be observed with 10 mM BAPTA in cells held for several minutes with low series resistance, where the cell is likely to be well dialyzed (Fig. 6). We conclude that strong buffering of cytoplasmic $Ca^{2+}$ does not eliminate $Ca^{2+}$-dependent inactivation.

$Ca^{2+}$-dependent inactivation still occurs after rundown of the whole-cell current to 20% of its initial value (Fig. 6), which should greatly reduce inactivation resulting from build-up of cytoplasmic $Ca^{2+}$. In six cells (with 1 or 10 mM EGTA) where the peak current ran down by $46 \pm 6\%$, time constants for inactivation during 60-ms pulses were $23 \pm 2$ ms initially and $22 \pm 3$ ms after rundown.

Parallel decreases of the whole cell calcium current and rate of inactivation were observed upon changing extracellular $Ca^{2+}$ from 10 mM to 1 mM (Fig. 7). In five cells tested at both concentrations, time constants for inactivation were $23 \pm 2$ ms in 10 mM $Ca^{2+}$ and $58 \pm 6$ ms in 1 mM $Ca^{2+}$. These effects were reversible, and thus not secondary to rundown (not shown). Longer prepulses in 1 mM $Ca^{2+}$ produce more

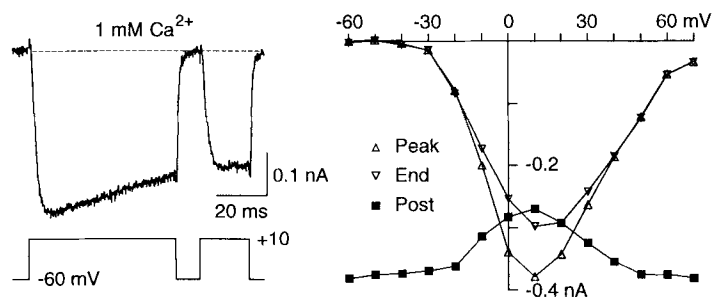

FIGURE 7. Inactivation of calcium current generated by a short pulse in 1 mM $[Ca^{2+}]_o$, with the same protocol as Fig. 1.

inactivation, as in 10 mM $Ca^{2+}$ or 10 mM $Ba^{2+}$. Preliminary results show that inactivation is not changed by decreasing $[Ba^{2+}]_o$ from 10 mM to 1 mM.

### Recovery from Inactivation

It might be supposed that recovery from $Ca^{2+}$-dependent inactivation would require removal of intracellular $Ca^{2+}$ following the end of the depolarization. This would predict that recovery from $Ca^{2+}$-dependent inactivation and recovery from voltage-dependent inactivation should differ qualitatively and quantitatively.

We examined the voltage and ion dependence of recovery from inactivation with the protocol of Fig. 8. For long pulses in $Ca^{2+}$, recovery is faster at more hyperpolarized potentials. Voltage steps directly to $-30$ or $-90$ mV do not markedly inactivate or facilitate the current. Fig. 9 compares results in three conditions: short prepulses in $Ca^{2+}$, long prepulses in $Ca^{2+}$, and long prepulses in $Ba^{2+}$. Recovery from inactivation is voltage dependent, even for short pulses in $Ca^{2+}$ where development of inactivation is $Ca^{2+}$ dependent.

Inactivation and recovery at $-30$ mV are examined more closely in Fig. 10. On these slower time scales, some degree of inactivation is apparent. The amount of inactivation at $-30$ mV varies among cells, probably since that voltage is near the threshold for inactivation, where slight voltage shifts would have substantial effects. In this cell, inactivation and recovery protocols converge in $\sim 1$ s after brief prepulses in $Ca^{2+}$ (Fig. 10 $A$ ), whereas $>2$ s are required after long pulses (Fig. 10, $B$ and $C$ ).



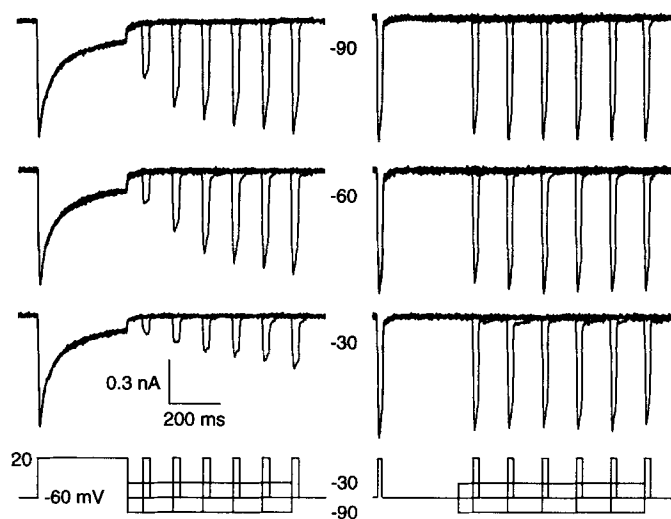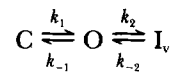FIGURE 8. Recovery from inactivation. At the left, the primary protocol used is illustrated for 360-ms prepulses to $+20$ mV in $Ca^{2+}$. After the prepulse, the cell was repolarized to $-30$, $-60$, or $-90$ mV for a variable time, and then a test pulse was given to $+20$ mV to test the amount of recovery. A similar protocol, shown at the right, was conducted to test for development or removal of inactivation by the steps to $-30$ or $-90$ mV. Design of the protocols for recovery from inactivation was complicated by several factors: ($a$) Inactivation was not complete, and the extent of inactivation measured during the prepulse could differ slightly from that measured at postpulses (due to inactivation during the postpulse). ($b$) When recovery was measured at voltages other than the holding potential, the maximal level of recovery was not necessarily the peak current during the prepulse. To correct for this, the maximal recovery level was defined as the point where recovery from inactivation and development of inactivation converge. That required the separate protocol to determine the time course of inactivation (or facilitation) at each voltage. ($c$) Rundown, which is exacerbated by long depolarizing steps, required that each current be normalized to the peak current during a prepulse. For the development of inactivation protocol, the prepulse had to be brief, and sufficient time had to be allowed for inactivation generated by the prepulse to recover.

Time constants for recovery from inactivation were measured from the protocols of Figs. 8–10 (Table I). At $-30$ mV, recovery is faster after a short prepulse in $Ca^{2+}$ than after longer pulses. The time constant of recovery is smaller at negative voltages, and the time constants at $-90$ mV are similar under all three conditions. We conclude that recovery from inactivation is voltage dependent, after both $Ca^{2+}$-dependent and voltage-dependent inactivation.

*Model*

The voltage-dependent inactivation seen in $Ba^{2+}$ can be described by a three-state sequential model with closed, open, and inactivated states:

$$C \underset{k_{-1}}{\overset{k_1}{\rightleftharpoons}} O \underset{k_{-2}}{\overset{k_2}{\rightleftharpoons}} I_v$$

Scheme 1

Activation kinetics were approximated with rate constants depending symmetrically on voltage, with voltage dependence chosen to reproduce the observed current—
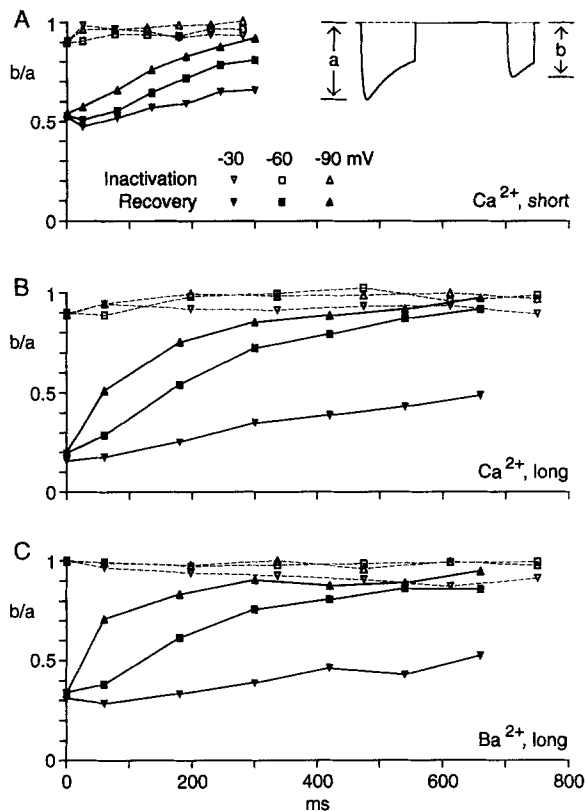


FIGURE 9. Voltage dependence of recovery from inactivation in three different conditions. The time course of inactivation (*open symbols, dashed lines*) and recovery from inactivation (*solid symbols and lines*) are compared at each voltage by the protocols of Fig. 8. Prepulses were 75 ms in $Ca^{2+}$ (*A*), 360 ms in $Ca^{2+}$ (*B*), or 360 ms in $Ba^{2+}$ (*C*). Values are peak currents during postpulses, normalized to the peak current during the prepulse (b/a; see inset). The points at time zero were measured at the end of the prepulse. The illustration of the protocol in the inset was calculated from the model (see below) with a 100-ms interval at $-60$ mV between the prepulse and postpulse.

voltage curve:

$$k_1 = 200\ e^{0.06(V-5)};\ k_{-1} = 200\ e^{-0.06(V-5)} \qquad (1, 2)$$

with units $s^{-1}$ and mV. Since inactivation in $Ba^{2+}$ follows activation of the current at negative voltages, microscopic inactivation need not depend on voltage, as macroscopic inactivation would be driven by the voltage dependence of activation. This would also explain the relative voltage insensitivity of the inactivation rate in $Ba^{2+}$

(Fig. 5). But for recovery from inactivation to be more rapid with hyperpolarization, the transition from the inactivated to the open state must be voltage dependent. For

$$k_2 = 4; k_{-2} = 0.5 \, e^{-0.03(V-5)} \tag{3, 4}$$

the voltage dependence of recovery from inactivation in $Ba^{2+}$ (Table I) is fit reasonably well.

Since $Ca^{2+}$-dependent inactivation survives strong $Ca^{2+}$ buffering (Fig. 6), we assume that $Ca^{2+}$ acts locally on the same channel through which it enters (see Discussion). This has the practical advantage of eliminating the need for detailed modeling of $Ca^{2+}$ diffusion and buffering in cytoplasm. We use the Goldman-
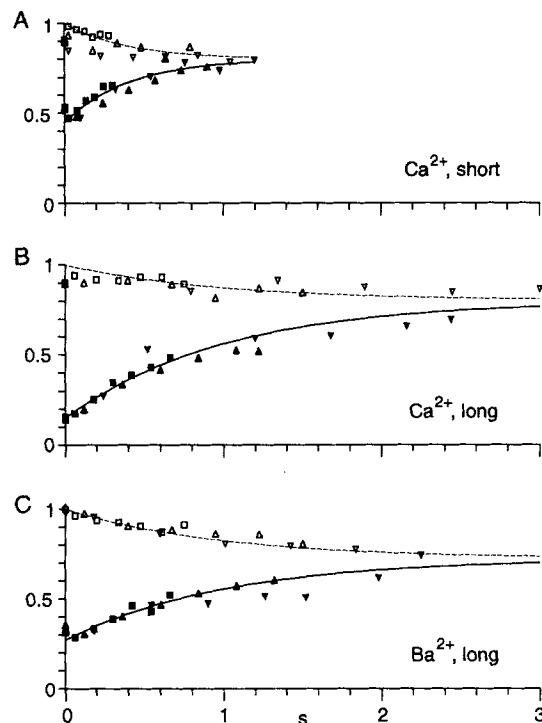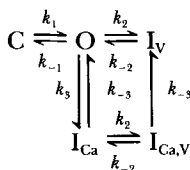


FIGURE 10. Recovery from inactivation at $-30$ mV. Symbols represent protocols of different length, and include data also plotted in Fig. 9. The curves drawn correspond to time constants of 400 ms ($A$) and 1 s ($B$ and $C$).

Hodgkin-Katz current equation to approximate the voltage dependence of $Ca^{2+}$ influx through an open channel (neglecting efflux), and we incorporate saturation of the channel by multiplying by a mass action factor:

$$G = fv/(1 - e^v) \tag{5}$$

where $f = [Ca^{2+}]_o/([Ca^{2+}]_o + K)$, $K = 2$ mM, $v = 2 \cdot V/25$, and the single-channel calcium current is proportional to $G$. Inactivation and recovery in $Ca^{2+}$ can now be described by a model where $Ca^{2+}$- and voltage-dependent inactivation proceed

independently:

$$C \underset{k_{-1}}{\overset{k_1}{\rightleftharpoons}} O \underset{k_{-2}}{\overset{k_2}{\rightleftharpoons}} I_V$$

$$k_3 \Big\Updownarrow k_{-3} \qquad k_{-3} \Big\Updownarrow$$

$$I_{Ca} \underset{k_{-2}}{\overset{k_2}{\rightleftharpoons}} I_{Ca,V}$$

Scheme 2

How was this model chosen? The existence of two distinct time constants for inactivation in $Ca^{2+}$ suggests a separate $Ca^{2+}$-dependent inactivated state, rather than

TABLE I

*Recovery from Inactivation*

| | Prepulse length (ms) | | |
|---|---|---|---|
| | $Ba^{2+}$ 360 | $Ca^{2+}$ 360 | $Ca^{2+}$ 75 |
| Recovery voltage | Time constant | | |
| *mV* | *ms* | | |
| Experimental data | | | |
| −90 | 110 ± 20 | 130 ± 20 | 110 ± 20 |
| −60 | 250 ± 40 | 230 ± 50 | 160 ± 20 |
| −30 | 710 ± 290 | 710 ± 300 | 370 ± 60 |
| Model | | | |
| −90 | 116 | 106 | 126 |
| −60 | 285 | 204 | 170 |
| −30 | 673 | 294 | * |

Experimental values are means (±SEM, $n = 5$) from linear regression of the logarithm of the fractional recovery vs. time. Time constants were measured from the protocols of Figs. 8–10, defining zero recovery as the current measured at the end of the prepulse, and full recovery as the point of convergence of the inactivation and recovery protocols. A cutoff of −2 ln units was used. Prepulses were given to the voltage generating peak inward current. For model simulations, time constants for recovery were calculated from single exponential fits to the return of channels to the closed state.

*Fit by two exponentials ($\tau = 72, 401$ ms) of equal amplitude.

an action of $Ca^{2+}$ to modulate the rates of voltage-dependent inactivation. This conclusion is greatly strengthened by the observation that intracellular trypsin selectively removes voltage-dependent inactivation (Obejero-Paz et al., 1991). Independent inactivation processes allow efficient movement of the initially $Ca^{2+}$-inactivated channels to a voltage-inactivated state, which makes recovery from inactivation similar after long depolarizations in $Ba^{2+}$ and $Ca^{2+}$ (Table I). Since $Ca^{2+}$-dependent inactivation is allowed only from the open channel, the model does not obey microscopic reversibility; flux around the cycle is driven by $Ca^{2+}$ entry.

For $k_3 = 70 \cdot G$ and $k_{-3} = 9$ in 10 mM $Ca^{2+}$, steps <100 ms to +20 mV produce predominantly $Ca^{2+}$-dependent inactivation, but the $I_V$ state is favored for long

pulses. These values are roughly equivalent to the statement that every $10^5$th $Ca^{2+}$ ion that enters prevents current flow through the channel for 110 ms.

This model produces reasonable fits to the voltage dependence of inactivation and recovery in $Ba^{2+}$ and $Ca^{2+}$ (Fig. 11, Table I), if kinetics are shifted 10 mV toward depolarized voltages in $Ca^{2+}$. The model predicts that recovery in $Ca^{2+}$ should require two exponentials, especially after short pulses, but the present data on recovery from inactivation are not adequate to resolve multiple time constants. The model also predicts less current and less inactivation in low $Ca^{2+}$ (Fig. 7).
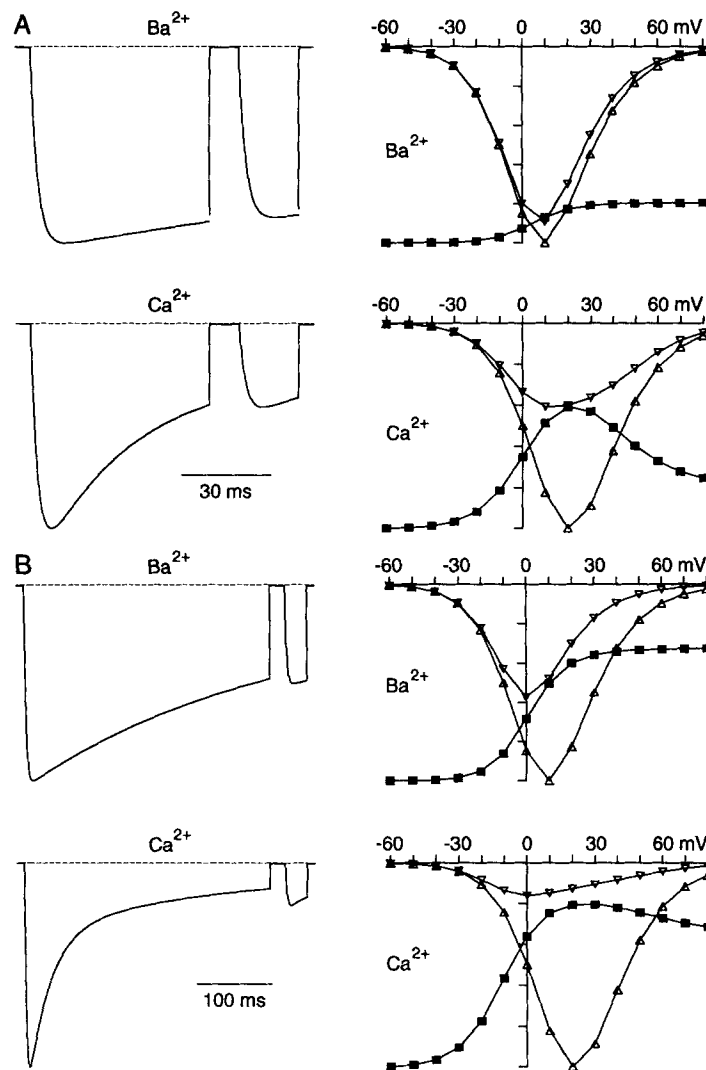


FIGURE 11. Calcium current inactivation calculated from Schemes 1 and 2. Currents and current–voltage relations are displayed as for Fig. 1 (*A*) and Fig. 2 (*B*). The absolute current levels are arbitrary.

Scheme 2 differs considerably from previous models of calcium current inactivation. Separate $Ca^{2+}$- and voltage-dependent inactivated states have been proposed previously (Yatani et al., 1983; Gutnick et al., 1989), but on those models $Ca^{2+}$- and voltage-dependent inactivation were mutually exclusive, not independent. Also, the model of Gutnick et al. (1989) places the site of $Ca^{2+}$ action at a distance from the channel. The surprising consequence is that $Ca^{2+}$-dependent inactivation depends not on $Ca^{2+}$ entry during the voltage step, but on the resting level of cytoplasmic $Ca^{2+}$. This predicts a monotonic dependence of $Ca^{2+}$-mediated inactivation on voltage, in agreement with their observations, but not with our data (Fig. 1) or most other data on calcium current inactivation.

### DISCUSSION

#### Two Components to Inactivation

The rapid component of inactivation in $Ca^{2+}$ is dependent on $Ca^{2+}$ entry. The slow component in $Ca^{2+}$, and essentially all inactivation in $Ba^{2+}$, are voltage dependent. Although similar conclusions have been drawn in other cases, the evidence here will be reviewed briefly.

Rapid inactivation is seen with $Ca^{2+}$ but not $Ba^{2+}$, parallels the amount of inward current, and is decreased at low $[Ca^{2+}]_o$. This is strong evidence for inactivation mediated by entry of $Ca^{2+}$.

The near monotonic increase in inactivation in $Ba^{2+}$ indicates voltage-dependent inactivation. However, the slight decrease in inactivation at positive voltages in $Ba^{2+}$ (Fig. 2) might suggest a contribution of current-dependent inactivation. For $Ba^{2+}$-dependent inactivation to be the predominant mechanism, voltage-dependent inactivation must be restricted to extreme positive voltages, since inactivation in $Ba^{2+}$ does not show a clear current dependence. That would require a steep voltage dependence for the microscopic inactivation process, despite the flat voltage dependence of the inactivation time constant in $Ba^{2+}$ (Fig. 5). We find this much less plausible than our model, where macroscopic inactivation in $Ba^{2+}$ is driven by the voltage dependence of the activation process.

Voltage-dependent inactivation also occurs with $Ca^{2+}$, since long pulses in $Ca^{2+}$ produce inactivation even at extreme positive potentials (Fig. 2), the time course of inactivation is fit by the sum of two exponentials (Fig. 4), and recovery from inactivation is similar after long pulses in $Ca^{2+}$ and $Ba^{2+}$ (Table I). Some $Ca^{2+}$-dependent inactivation might occur at extreme positive potentials, as some $Ca^{2+}$ entry is expected even positive to the reversal potential. However, we calculate that $Ca^{2+}$ influx at $+70$ mV is $<8\%$ of the peak current at $+20$ mV, either from the Goldman-Hodgkin-Katz current equation (Fig. 11), or from the Almers and McCleskey (1984) model for calcium channel permeation, assuming activation kinetics as in Eqs. 1 and 2 above.

#### The Site of $Ca^{2+}$ Action in $Ca^{2+}$-dependent Inactivation

Gutnick et al. (1989) calculated that high concentrations of BAPTA buffer $Ca^{2+}$ within microseconds further than a fraction of a micrometer from the channel. This suggests that $Ca^{2+}$ acts either at relatively high concentration in the immediate vicinity of the

channel (Chad and Eckert, 1984), or at low concentration throughout the cell (Gutnick et al., 1989).

Inactivation resulting from increases in bulk cytoplasmic $Ca^{2+}$ should be prevented by intracellular EGTA or BAPTA, as found for invertebrate neurons (Eckert and Chad, 1984; Gutnick et al., 1989). However, this is less clear for calcium currents of vertebrate smooth muscle (Ganitkevich et al., 1987; Katzka and Morad, 1989). Our observation that BAPTA slows, but does not eliminate, $Ca^{2+}$-dependent inactivation suggests that $Ca^{2+}$ acts at a site where BAPTA buffers $Ca^{2+}$ transients only partially. This would place the site of action outside the channel pore (which should be inaccessible to BAPTA) but within ~0.1 μm of the channel (Gutnick et al., 1989). An obvious possibility is binding to a cytoplasmic domain of the channel protein.

Attempts to mimic inactivation by raising $[Ca^{2+}]_i$ have produced inconsistent results. Inhibition of calcium currents by ~100 nM $[Ca^{2+}]_i$ has been reported (Byerly and Moody, 1984; Dupont et al., 1986; Ohya et al., 1988), but higher concentrations were required in other studies (Plant et al., 1983; Gutnick et al., 1989). These discrepancies may result in part from difficulties in maintaining a defined $[Ca^{2+}]_i$ in dialyzed cells (Byerly and Moody, 1984). Release of "caged" $Ca^{2+}$ at micromolar levels by photolysis of buffers rapidly ($\tau \approx 7$ ms) but partially reduced calcium current in sensory neurons (Morad et al., 1988), but actually enhanced calcium current in cardiac cells (Gurney et al., 1989). Cardiac calcium channels in planar bilayers are rapidly blocked by $Ca^{2+}$, with an apparent dissociation constant of 4 mM and no change in gating kinetics (Rosenberg et al., 1988). These effects are difficult to relate to the normal inactivation process.

It has been proposed that $Ca^{2+}$-dependent inactivation results from a dephosphorylation reaction (Chad and Eckert, 1986; Kalman et al., 1988). However, the rapid rates of inactivation (~25 ms) and recovery (~120 ms) at room temperature are at the upper limit of the rates expected for phosphatase or kinase reactions. It is also possible that enzymatic regulation of calcium channel availability does occur, but is distinct from the rapid inactivation process discussed here.

Mazzanti and DeFelice (1990) and Yue et al. (1990) recently reported $Ca^{2+}$-dependent inactivation at the single-channel level, with cell-attached patches on cardiac cells. A channel inactivates slowly with $Ba^{2+}$, even when $Ca^{2+}$ is entering through all of the other calcium channels in the cell (Mazzanti and DeFelice, 1990). This is conclusive evidence for local, channel-by-channel inactivation.

### Role of Calcium Channel Inactivation

Since intracellular $Ca^{2+}$ is the primary signal for muscle contraction in cardiac and smooth muscle, $Ca^{2+}$-dependent inactivation could serve as a potent negative feedback mechanism for regulation of contraction. This is particularly true in arterial smooth muscle, where $Ca^{2+}$ entry normally occurs in response to slow, graded depolarization rather than action potentials (Nelson et al., 1990). Given the strong driving force for $Ca^{2+}$ in the critical voltage region (-40 to -55 mV), the large single-channel currents could produce strong $Ca^{2+}$-dependent inactivation on a channel-by-channel basis. Such voltages might also produce significant voltage-dependent inactivation, especially if slow inactivation occurs (Schouten and Morad, 1989).

### REFERENCES

Almers, W., and E. W. McCleskey. 1984. Non-selective conductance in calcium channels of frog muscle: calcium selectivity in a single-file pore. *Journal of Physiology.* 353:585–608.

Brown, A. M., K. Morimoto, Y. Tsuda, and D. L. Wilson. 1981. Calcium current-dependent and voltage-dependent inactivation of calcium channels in *Helix aspersa. Journal of Physiology.* 320:193–218.

Byerly, L., and J. W. Moody. 1984. Intracellular calcium ions and calcium current in perfused neurones of the snail *Lymnea stagnalis. Journal of Physiology.* 352:637–652.

Carbone, E., and D. Swandulla. 1989. Neuronal calcium channels: kinetics, blockade and modulation. *Progress in Biophysics and Molecular Biology.* 54:31–58.

Chad, J. E., and R. Eckert. 1984. Calcium domains associated with individual channels can account for anomalous voltage relations of Ca-dependent responses. *Biophysical Journal.* 45:993–999.

Chad, J. E., and R. Eckert. 1986. An enzymatic mechanism for calcium current inactivation in dialyzed *Helix* neurons. *Journal of Physiology.* 378:31–51.

Dupont, J. L., J. L. Bossu, and A. Feltz. 1986. Effect of internal calcium concentration on calcium currents in rat sensory neurones. *Pflügers Archiv.* 406:433–435.

Eckert, R., and J. E. Chad. 1984. Inactivation of Ca channels. *Progress in Biophysics and Molecular Biology.* 44:215–267.

Eckert, R., and D. L. Tillotson. 1981. Calcium mediated inactivation of the calcium conductance in caesium loaded giant neurones of *Aplysia californica. Journal of Physiology.* 314:265–280.

Ganitkevich, V. Ya., M. F. Shuba, and S. V. Smirnov. 1987. Calcium-dependent inactivation of potential-dependent calcium inward current in an isolated guinea pig smooth muscle cell. *Journal of Physiology.* 392:431–449.

Giannattasio, B., S. W. Jones, and A. Scarpa. 1989. $Ca^{2+}$- and voltage-dependent inactivation of calcium currents in the A7r5 smooth muscle derived cell line. *Physiologist.* 32:209. (Abstr.)

Giannattasio, B., S. W. Jones, and A. Scarpa. 1990. Inactivation of calcium current in the A7r5 smooth muscle cell line is calcium- and voltage-dependent. *Biophysical Journal.* 57:522a. (Abstr.)

Gurney, A. M., P. Charnet, J. M. Pye, and J. Nargeot. 1989. Augmentation of cardiac calcium current by flash photolysis of intracellular caged-$Ca^{2+}$ molecules. *Nature.* 341:65–68.

Gutnick, M. J., H. D. Lux, D. Swandulla, and H. Zucker. 1989. Voltage-dependent and calcium-dependent inactivation of calcium channel current in identified snail neurones. *Journal of Physiology.* 412:197–220.

Jmari, K., C. Mironneau, and T. Mironneau. 1986. Inactivation of calcium channel current in rat uterine smooth muscle: evidence for calcium and voltage mediated mechanisms. *Journal of Physiology.* 380:111–126.

Jones, S. W., and T. N. Marks. 1989. Calcium current in bullfrog sympathetic neurons. II. Inactivation. *Journal of General Physiology.* 94:169–182.

Kalman, D., P. H. O'Lague, C. Erxleben, and D. L. Armstrong. 1988. Calcium-dependent inactivation of the dihydropyridine-sensitive calcium channels in GH₃ cells. *Journal of General Physiology.* 92:531–548.

Kass, R. S., and M. C. Sanguinetti. 1984. Inactivation of calcium channel current in the calf cardiac Purkinje fiber. Evidence for voltage- and calcium-mediated mechanisms. *Journal of General Physiology.* 84:705–726.

Katzka, D. A., and M. Morad. 1989. Properties of calcium channels in guinea-pig gastric myocytes. *Journal of Physiology.* 413:175–197.

Kimes, B. W., and B. L. Brandt. 1976. Characterization of two putative smooth muscle cell lines from rat thoracic aorta. *Experimental Cell Research.* 98:349–366.

Lee, K. S., E. Marban, and R. W. Tsien. 1985. Inactivation of calcium channels in mammalian heart cells: joint dependence on membrane potential and intracellular calcium. *Journal of Physiology.* 364:395–411.

Marks, T. N., G. R. Dubyak, and S. W. Jones. 1990. Calcium currents in the A7r5 smooth muscle-derived cell line. *Pflügers Archiv.* 417:433–439.

Mazzanti, M., and L. J. DeFelice. 1990. Ca channel gating during cardiac action potentials. *Biophysical Journal.* 58:1059–1065.

McCarthy, R. T., and C. J. Cohen. 1989. Nimodipine block of calcium channels in rat vascular smooth muscle cell lines. Exceptionally high-affinity binding in A7r5 and A10 cells. *Journal of General Physiology.* 94:669–692.

Morad, M., N. W. Downes, J. H. Kaplan, and H. D. Lux. 1988. Inactivation and block of calcium channels by photo-released $Ca^{2+}$ in dorsal root ganglion neurons. *Science.* 241:842–844.

Nelson, M. T., J. B. Patlak, J. F. Worley, and N. B. Standen. 1990. Calcium channels, potassium channels, and voltage dependence of arterial smooth muscle tone. *American Journal of Physiology.* 259:3–18.

Obejero-Paz, C. A., S. W. Jones, and A. Scarpa. 1991. Calcium currents in the A7r5 smooth muscle-derived cell line. Increase in current and selective removal of voltage-dependent inactivation by intracellular trypsin. *Journal of General Physiology.* In press.

Obejero-Paz, C., T. N. Marks, S. W. Jones, G. R. Dubyak, and A. Scarpa. 1990. Kinetics of activation of L-type calcium channels in the A7r5 smooth muscle cell line. *Biophysical Journal.* 57:522a. (Abstr.)

Ohya, Y., K. Kitamura, and H. Kuriyama. 1988. Regulation of calcium current by intracellular calcium in smooth muscle cells of rabbit portal vein. *Circulation Research.* 62:375–383.

Plant, T. D., N. B. Standen, and T. A. Ward. 1983. The effect of injection of calcium ions and calcium chelators on calcium channel inactivation in *Helix* neurones. *Journal of Physiology.* 334:189–212.

Rosenberg, R. L., P. Hess, and R. W. Tsien. 1988. Cardiac calcium channels in planar lipid bilayers. L-type channels and calcium-permeable channels open at negative membrane potentials. *Journal of General Physiology.* 92:27–54.

Satin, L. S., and D. L. Cook. 1989. Calcium current inactivation in insulin secreting cells is mediated by calcium influx and membrane depolarization. *Pflügers Archiv.* 414:1–10.

Schouten, V. J. A., and M. Morad. 1989. Regulation of $Ca^{2+}$ current in frog ventricular myocytes by the holding potential, c-AMP and frequency. *Pflügers Archiv.* 415:1–11.

Yatani, A., D. L. Wilson, and A. M. Brown. 1983. Recovery of Ca currents from inactivation: the roles of Ca influx, membrane potential, and cellular metabolism. *Cellular and Molecular Neurobiology.* 3:381–395.

Yue, D. T., P. H. Backx, and J. P. Imredy. 1990. Calcium-sensitive inactivation in the gating of single calcium channels. *Science.* 250:1735–1738.